An abrupt drop of coherence of the lower kilo-Hz QPO in 4U1636-536

D. Barret, J. F. Olive, M. C. Miller

Mon. Not. R. Astron. Soc. **361,** 855–860 (2005) doi:10.1111/j.1365-2966.2005.09214.x

An abrupt drop in the coherence of the lower kHz quasi-periodic oscillations in 4U 1636−536

Didier Barret,[1]★ Jean-Francois Olive[1] and M. Coleman Miller[2]
[1]*Centre d'Etude Spatiale des Rayonnements, CNRS/UPS, 9 Avenue du Colonel Roche, 31028 Toulouse Cedex 04, France*
[2]*Department of Astronomy, University of Maryland, College Park, MD 20742-2421*

Accepted 2005 May 18. Received 2005 May 18; in original form 2005 March 17

ABSTRACT

Using archival data from the *Rossi X-ray Timing Explorer* (*RXTE*), we study in a systematic way the variation of the quality factor ($Q = \nu/\Delta\nu$, $\Delta\nu$, full width at half maximum) and amplitude of the lower and upper kHz quasi-periodic oscillations (QPOs) in the low-mass X-ray binary 4U 1636−536, over a frequency range from ∼550 to ∼1200 Hz. When represented in a quality factor versus frequency diagram, the upper and lower QPOs follow two different tracks, suggesting that they are distinct phenomena, although not completely independent because the frequency difference of the two QPOs, when detected simultaneously, remains within ∼60 Hz of half the neutron star spin frequency (at $\nu_{\rm spin} = 581$ Hz). The quality factor of the lower kHz QPO increases with frequency up to a maximum of $Q \approx 200$ at $\nu_{\rm lower} \approx 850$ Hz, then drops precipitously to $Q \approx 50$ at the highest detected frequencies $\nu_{\rm lower} \approx 920$ Hz. A ceiling of the lower QPO frequencies at 920 Hz is also clearly seen in a frequency versus count rate diagram. At the same time, the quality factor of the upper kHz QPO increases steadily from $Q \sim 5$ to ∼15 all the way to $\nu_{\rm upper} \approx 1150$ Hz, which is the highest detectable QPO frequency. The rms amplitudes of both the upper and lower kHz QPOs decrease steadily towards higher frequencies.

The quality factor provides a measure of the coherence of the underlying oscillator. For exponentially damped sinusoidal shots, the highest Q observed corresponds to an oscillator coherence time of $1/\pi\Delta\nu \sim 0.1$ s. All existing QPO models face challenges in explaining such a long coherence time and the significantly different behaviours of the quality factors of the upper and lower QPOs reported here. It is therefore difficult to be certain of the implications of the abrupt change in the lower QPO at ∼850 Hz. We discuss various possible causes, including that the drop in coherence is ultimately caused by effects related to the innermost stable circular orbit.

Key words: accretion, accretion discs – stars: individual: 4U 1636−536 – stars: neutron – X-rays: stars.

1 INTRODUCTION

Following the discovery with *RXTE* in 1996 of kHz quasi-periodic oscillations (QPOs) in neutron star low-mass X-ray binaries (LXMBs), it was immediately realized that they offer unique probes of the strongly curved space–time around compact stars, possibly providing ways of testing some of the most fundamental predictions of general relativity (GR) in the strong field regime (e.g. van der Klis 2005). One of the key predictions of strong gravity GR is that there exists a region around sufficiently compact stars within which no stable circular orbital motion is possible. In a Schwarzschild geometry, the radius of the innermost stable circular orbit (ISCO) is $6GM/c^2$ (e.g. Bardeen, Press & Teukolsky 1972; see also Kluźniak & Wagoner 1985), which is greater than the radii of neutron stars constructed with most modern high-density equations of state (see Akmal, Pandharipande & Ravenhall 1998). Prior to the launch of *RXTE*, it was suggested that the ISCO might induce a frequency cut-off in the power density spectrum (Kluźniak, Michelson & Wagoner 1990). After the discovery of kHz QPOs, it was proposed that signatures of the ISCO could include a frequency saturation of kHz QPOs with increasing mass accretion rate, or a drop in the quality factor and rms amplitude of kHz QPOs as they approach a limiting frequency (Miller, Lamb & Psaltis 1998).

An apparent frequency saturation with increasing count rate was in fact claimed for the neutron star LMXB 4U 1820–30

★E-mail: Didier.Barret@cesr.fr

(Smale, Zhang & White 1997; Zhang et al. 1998). This was disputed due to concern that the count rate might not be an accurate measure of mass accretion rate, and it was proposed that the quantity S_a (a measure of the location of an atoll source on an X-ray colour–colour diagram) would be more representative (Méndez et al. 1999; Méndez 2002). Additional analyses of data integrated over *RXTE* orbits show frequency saturation against many other measures of mass accretion rate, including S_a (e.g. Kaaret et al. 1999; Bloser et al. 2000). However, short-term variations of the frequency are important, and there is not a one-to-one correlation between S_a and the QPO frequency (e.g. Di Salvo, Méndez & van der Klis 2003), suggesting that S_a might not be a precise indicator of mass accretion rate after all. Therefore, although the ISCO interpretation in 4U 1820–30 remains a possibility, its status is uncertain.

The large *RXTE* archive now makes possible searches for systematic correlations between frequency, quality factor and amplitude in unbiased data sets. For example, our analysis of the neutron star LMXB 4U 1608−52 revealed a positive correlation between the frequency $\nu_{\rm lower}$ of the lower frequency kHz QPO and its quality factor, up to a maximum of about $Q = 200$, beyond which the two quantities were anticorrelated (Barret et al. 2005). Such a result places stringent constraints on models, especially those relating QPOs to orbiting clumps.

Motivated by this result, we investigate the properties of QPOs in the similar system 4U 1636−536. This system is ideal for several reasons: its kHz QPOs are strong, their frequencies vary over a wide range, and 4U 1636−536 has been observed extensively with *RXTE*. Its kHz QPO properties have been studied as a function of count rate, luminosity, energy spectral parameters and other quantities (e.g. Zhang, Lapidus & White 1996a; Zhang et al. 1996b; Wijnands et al. 1997; Méndez, van der Klis & van Paradijs 1998b; Jonker, Méndez & van der Klis 2000, 2002; Di Salvo et al. 2003; Misra & Shanthi 2004).

Here we focus on the quality factor and amplitude of the kHz QPOs, which we analyse systematically by putting together all the available observations of the *RXTE* archive to date. We discuss our data reduction procedure in Section 2. We discuss the possible implications of our results in Section 3.

2 DATA REDUCTION PROCEDURE

We have retrieved all the Proportional Counter Array science event files with time resolution better than or equal to 250 μs. Only data files with exposure times larger than 600 s are considered here. The data set covers the period from 1996 April to 2004 September. No filtering on the raw data is performed, which means that all photons are used in the analysis, only time-intervals containing X-ray bursts are removed. We have computed Leahy-normalized Fourier power density spectra (PDS) between 1 and 2048 Hz over 8-s intervals (with a 1-Hz resolution).

2.1 QPO identification

A PDS which is the average of all the 8-s PDS over a continuous data segment is first computed; the typical length of the segment is ∼4500 s, i.e. comparable to the orbital period of the *RXTE* spacecraft. The segment-averaged PDS is then searched for a QPO using a scanning technique which looks for peak excesses above the Poisson counting noise level (see Boirin et al. 2000). Because at the lowest frequency, typically ∼400 Hz, QPOs become broad features, merging with broad noise components (e.g. Olive, Barret & Gierliński 2003), they are difficult to detect with an automatic procedure. For this reason, the QPO search is restricted to frequencies above 500 Hz. The detection threshold for the QPO is 8σ in a given segment. Of the 631 event files analyzed, 201 matched our selection criteria.

Having located the strongest QPO peak in each segment-averaged PDS, we now wish to get an estimate of the quality factor of the QPO, reducing as much as possible the contribution of the long-term frequency drifts. We therefore follow the QPO on the shortest possible time-scales permitted by the data statistics. We divide each continuous data segment into N intervals, and search for a QPO within a 50-Hz window around the frequency of the QPO in the segment-averaged PDS. The possible interval durations considered are 16, 32, 64, 128, 256, 512 and 1024 s. The shortest usable integration time is then estimated such that the QPO is detected (above 4σ) in at least 80 per cent of the N intervals (a linear interpolation is used to estimate the QPO frequency in the remaining intervals). The N PDS are then (frequency) shifted to the mean QPO frequency over the segment and averaged (Méndez et al. 1998a). The segment-averaged QPO profile is then fitted over a 100 Hz frequency range (50 Hz on each side of the QPO peak) with a Lorentzian having three parameters (amplitude, frequency and $\Delta\nu$) plus a constant representing the counting-statistics noise level, following the method described in Barret et al. (2005). The uncertainties in the fitted parameters are computed such that $\chi^2 = \chi^2_{\rm min} + 1$ for variation of one single parameter.

The quality factor of the strongest QPOs ($Q_{\rm seg}$), so obtained, is represented in Fig. 1. This figure shows two distinct branches. For

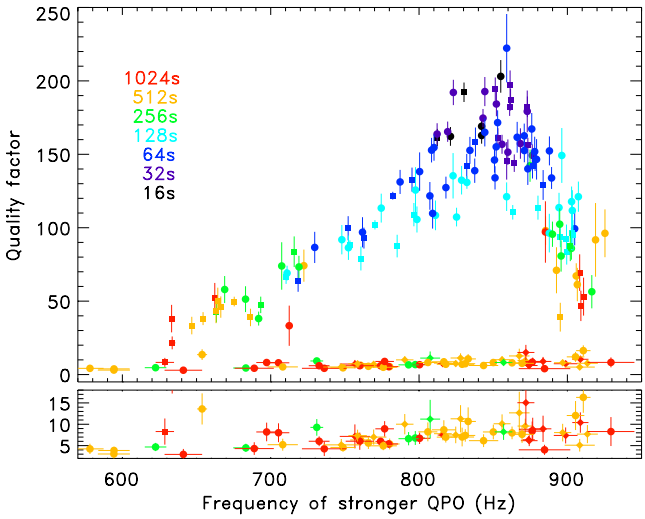

Figure 1. Top panel: quality factor versus frequency of the stronger 201 QPOs detected from 4U 1636−536. There are clearly two classes of QPOs showing up in that figure; one for which Q steadily increases between 600 and 850 Hz and then decreases afterwards (this branch contains all identified lower QPOs, filled squares), and another class of QPOs which includes those detected with the longest integration times, and which seems to show a positive correlation between Q and frequency between 600 Hz and 900 Hz (it includes all identified upper QPOs, filled diamonds). Segments for which only one QPO was detected are shown with filled circles. They are mostly found on the lower QPO branch. Different colours (this figure is available in colour in the online version of this journal on *Synergy*) correspond to different integration times for the PDS, ranging from 16 to 1024 s. Bottom panel: a blow-up of the y-axis suggesting that for the upper QPO, a positive correlation exists between Q and frequency over the frequency range ∼600 to 930 Hz (the Spearman correlation coefficient is 0.35 corresponding to a null-hypothesis probability of $3.4\,10^{-7}$, see also Fig. 4).

the main branch $Q_{\rm seg}$ increases with frequency up to a maximum (∼850 Hz) beyond which a sharp decrease is observed. A bottom track is seen at the bottom of the plot. It includes broader QPOs, detected only on the longest integration times. There is a trend for $Q_{\rm seg}$ of these QPOs to increase with frequency along the track.

To determine whether the strongest QPO detected is the lower or the upper kHz QPO, the shifted and averaged PDS for each segment is searched for a second QPO using the same scanning technique between 500 and 1300 Hz. A second QPO is detected if its significance above the counting noise level is greater than 4σ (following the method described in Boirin et al. 2000). With this procedure, we directly detect a weaker upper kHz QPO in 53 segments: all segments marked with filled squares in Fig. 1 are located on the upper branch. We also detect a weaker lower kHz QPO in 24 segments: all of these segments marked with filled diamonds are located on the bottom branch of Fig. 1. From this we conclude that the upper curvy branch ($Q_{\rm seg} > 15$) is the lower QPO branch, whereas the bottom track ($Q_{\rm seg} < 15$) is the upper QPO branch. As can be seen from Fig. 1, many segments including a single QPO (filled circles) (i.e. in which the second one is not detected above 4σ) are found on the lower QPO branch, hence contain lower QPOs. This demonstrates that our method, applied to a large data set, provides a way to identify kHz QPOs, based on the frequency dependency of their Q values. Alternative methods do exist, as for instance the one based on frequency correlations between kHz QPOs and features at lower frequencies <100 Hz (van Straaten, van der Klis & Méndez 2003).

Note that the upper QPO is detected as the strongest QPO when its frequency is between ∼600 and 930 Hz. This means that there are no segments of data where the upper QPO has a frequency larger than 930 Hz and a significance larger than $8\,\sigma$. Obviously, this does not mean that the upper QPO does not reach frequencies higher than 930 Hz, as we will see below. Over a limited frequency range (770 to 920 Hz), and for a limited data set, the same trends for the quality factor of both QPOs were present in the 4U 1636−536 data analysed in Di Salvo et al. (2003).

In the above analysis, the integration time used in estimating $Q_{\rm seg}$ is minimized and therefore is not the same for all the PDS. It ranges from 16 to 1024 s, leading to a potential bias, because weaker or broader QPOs will require longer integration times to be detected, and hence will suffer from a larger broadening due to a larger frequency drift within the interval. As shown in Fig. 1, the highest $Q_{\rm seg}$ are indeed detected on the shortest time-scales. We have verified for both the upper and lower QPOs that the same trend is observed for their quality factors when the PDS integration time is not optimized, but instead is the same for all segments, e.g. 1024 s. The upper and lower branches are still clearly distinct; the main difference being that the upper one (which contains segments for which the PDS integration time could be reduced to 16 s in some cases) is shifted downwards to smaller $Q_{\rm seg}$ (with a maximum around 100). This is expected as the QPO width includes now a larger contribution from the long-term frequency drifts, leading to smaller $Q_{\rm seg}$.

More than 7900 individual PDS are used in the present analysis, amounting for about 840 ks of QPOs. The detected QPO frequencies in the individual PDS are plotted against total source count rates in Fig. 2 for the lower QPO as identified above (those corresponding to $Q_{\rm seg} > 15$). This figure shows the so-called parallel track phenomenon (Méndez et al. 1999; van der Klis 2001). The tracks flatten at high count rates. Note that there is a clear ceiling in frequency (around 920 Hz) above which no QPOs are detected, whatever the source count rate is.

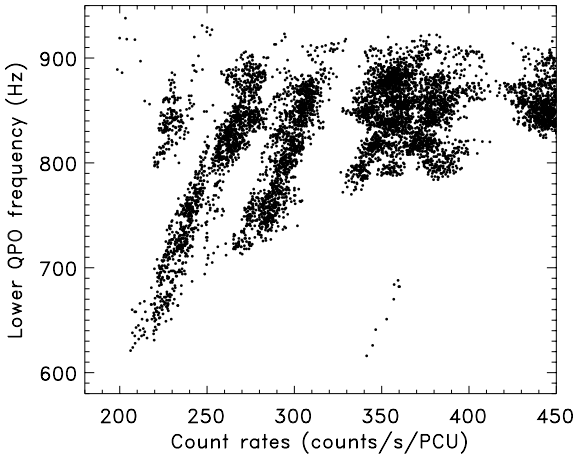

Figure 2. Lower QPO frequencies versus count rates (normalized by the number of PCA units operating). Note the clean limitation in frequency around 920 Hz seen for the lower QPOs.

2.2 *Q* and amplitude versus frequency

In order to get a better estimate of the Q versus frequency dependency, we now divide the individual PDS in two classes, those contributing to $Q_{\rm seg}$ larger than 15 (the lower QPOs) and those associated with $Q_{\rm seg}$ smaller than 15 (the upper QPOs). The lower QPO spans a frequency range from 620 to 920 Hz. We divide this range with steps of 15 Hz. In each frequency bin (e.g. 620–635 Hz), all the individual PDS whose strong QPO frequency fall in the bin are shifted-and-added to a mean QPO frequency measured within the bin. The lower QPO is then fitted, and its quality factor and rms amplitude estimated from the fit. An upper QPO is always present. However, it is broad ($\gtrsim$70 Hz) and therefore difficult to fit. We could obtain reliable fit parameters for 18 segments. We repeat the analysis for the PDS associated with $Q_{\rm seg}$ less than 15, but with frequency bins of 30 Hz (as we have less individual PDS involved). A significant fit for the lower QPO is obtained on only two occasions.

Figs 3 and 4 show the quality factor and rms amplitude of the lower and upper QPOs as estimated with our analysis. The patterns seen for Q in Fig. 1 are evident, but this time with much less scatter.

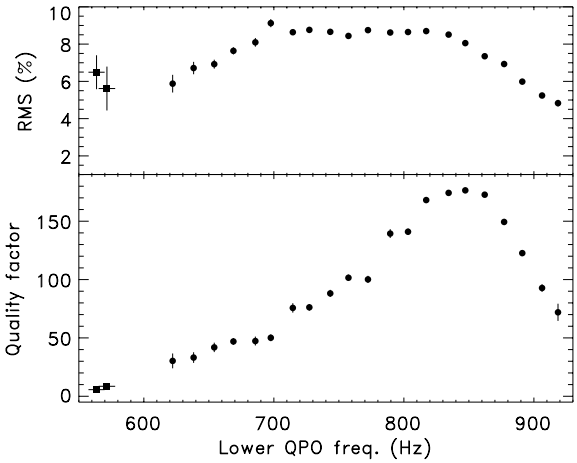

Figure 3. The rms amplitude and quality factor of the lower kHz QPO of 4U 1636−536, as measured every 15 Hz. Points marked with filled squares have been obtained from fitting the lower QPO in segments where the upper QPO was the strongest.

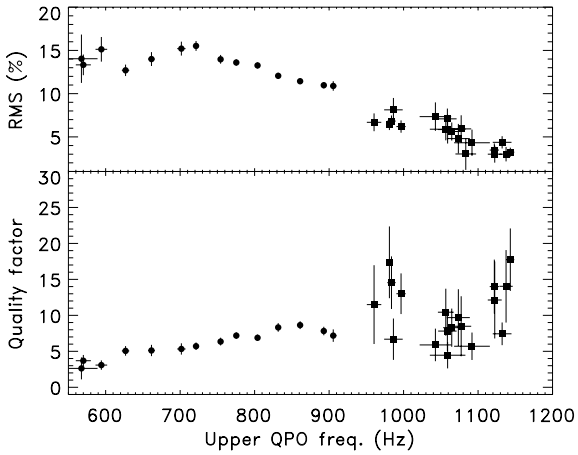

Figure 4. The rms amplitude and quality factor of the upper kHz QPO of 4U 1636−536 as derived every 30 Hz. Points marked with filled squares have been obtained from fitting the upper QPO in segments where the lower QPO was the strongest.

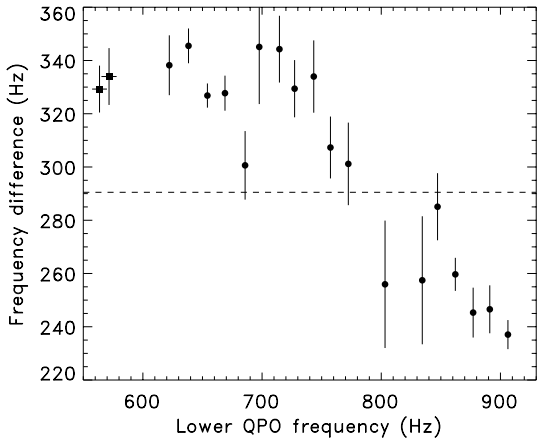

Figure 5. The frequency difference between the upper and lower QPOs (filled squares correspond to points when the upper is the strongest QPO of the two, filled circles are those for which the lower is the strongest QPO of the two). Half the neutron star frequency is indicated with a dashed line at 290 Hz. The frequency difference remains within ∼60 Hz of half the spin frequency, suggesting that the spin plays a role in setting up the frequencies.

The most striking features of these two figures are the following: the quality factor of the lower QPO shows a smooth increases with frequency, reaching a maximum at 850 Hz, and decreasing sharply afterwards. On the other hand, the quality factor of the upper QPO smoothly increases up to 850 Hz, with no evidence for a drop afterwards (note however that only the narrower signals have been fitted and the error bars are relatively large). Finally, the rms amplitude of both QPOs decreases steadily at the highest frequencies. The upper QPO is detected close to the rms detection threshold of our analysis: typically ∼2.0 per cent rms (3σ) for a typical width of 50–100 Hz. Therefore its non-detection at frequencies higher than ∼1150 Hz could be due to a lack of sensitivity.[1] On the other hand, for the lower and narrower QPO, our detection threshold is closer to ∼1.0 per cent rms. This value is less than one fourth of the rms measured for its highest frequency at ∼920 Hz, thus providing further support to the idea that the lower QPO truly disappears.

2.3 Relation with spin

From X-ray burst oscillations, the spin frequency ($\nu_{\rm spin}$) of the neutron star is thought to be 581 Hz (Strohmayer & Markwardt 2002). As shown in Fig. 5, when we detect both QPOs in the above analysis, the frequency difference remains within ∼60 Hz of half the spin frequency, with a mean value around 300 Hz (our results are fully consistent with the one presented in Jonker et al. 2002). It is interesting to note that the peak of coherence is reached when the frequency difference is the closest to half the spin frequency.

3 DISCUSSION

We have studied systematically the quality factor and rms amplitude of the kHz QPOs detected from 4U 1636−536 with *RXTE*. Using a shift-and-add technique to minimize the contribution of the long-term frequency drift to the measured width of the QPO, we have shown that the lower and upper kHz QPOs follow two different tracks in a diagram of quality factor versus frequency.

[1] Note however that if the lower QPO frequency is limited to ∼920 Hz with the frequency difference between the upper and lower QPOs remaining less than half the spin frequency, as suggested in Fig. 5, the upper QPO frequency is not expected to reach values higher than ∼1150–1200 Hz.

The most striking result reported here is the frequency evolution of the coherence of the lower kHz QPOs. The coherence of the lower QPO shows a clear increase from 600 to 850 Hz, then a sharp decrease in coherence to the maximum observed frequency of about 920 Hz (see Fig. 3). The same behaviour was suggested from the 4U 1608−522 data (Barret et al. 2005). The rms amplitude remains roughly constant between 600 and 820 Hz and then decreases smoothly. A similar dependence of rms amplitude on frequency has been reported for other systems (Méndez, van der Klis & Ford 2001). The quality factor of the lower kHz QPO reaches $Q = 222 \pm 24$ at 860 Hz on 2000 August 12. This value, as well as the frequency at which it occurs, is remarkably similar to the one observed previously from 4U 1608−522 (Berger et al. 1996; Barret et al. 2005). For exponentially damped sinusoidal shots, this high Q value corresponds to an oscillator coherence time of $1/\pi\Delta\nu \sim 0.1$ s, or about 70 cycles. As discussed in Barret et al. (2005), this long coherence time, as well as the different behaviours of the lower and upper QPOs (see Figs 1, 3 and 4), pose severe constraints on *all* existing QPO models. These findings are particularly constraining on models involving orbiting clumps; the reason being that clumps, left alone in the disc, will be sheared by differential rotation in just a few cycles. For the clumps to survive against tidal shear would require that some local forces, unidentified so far, can keep them together.

Our analysis of 4U 1636−536 and 4U 1608−52, combined with previous results on kHz QPOs, produces an apparent paradox. The different quality factor dependences of the two QPOs might seem to imply that the mechanisms for generating the two QPOs are decoupled from each other. However, it has been shown in many systems that the separation frequency between the lower and upper kHz QPOs is close to the stellar spin frequency or half the spin frequency (see, e.g. Wijnands et al. 2003, for a discussion related to the accretion-powered millisecond pulsar SAX J1808−3658). For 4U 1636−536, the frequency difference we measured between the two QPOs is also close to half the neutron star spin frequency (see Fig. 5). This would seem to suggest that the two kHz QPOs are linked to each other, and that the spin plays a role in producing at least one of the QPOs. Resolution of these apparently discrepant observations will be an important task for QPO models.

Despite the uncertainties about the origin of the QPOs, some relatively model-independent conclusions can be drawn. Let us first consider what governs the frequencies and coherences of the QPOs. There are three regions in the system that can produce emission: the cool disc, the hot corona above the disc, and the boundary layer of accretion on to the star (e.g. Barret et al. 2000). In fact, the presence of QPOs in the high-energy emission $E > 20$ keV (van der Klis 2005) requires that at least some emission come from other than the $kT \sim 1$–2 keV disc. However, this does *not* mean that the observed frequency *originates* in the corona or boundary layer. For example, oscillations in the disc could modify the temperature or optical depth of the corona, or the accretion rate on to the star, leading to modulation of the high-energy emission. Indeed, there are no easily conceivable mechanisms by which highly coherent oscillations could be generated primarily in the corona, let alone in the turbulent boundary layer. In contrast, the disc offers many possibilities for characteristic frequencies, from orbital or epicyclic frequencies to oscillation modes. We therefore consider it highly likely that the frequencies of the QPOs are determined in the disc, even if the emission is produced elsewhere.

Now consider the implications of a sharp change in QPO behaviour that occurs reproducibly at a given frequency. Such a change implies that there is something special about the disc when that frequency is reached. If this change occurred only once, or just at a single count rate, it could be that for complicated reasons the disc undergoes a change of state. In the case of 4U 1636−536, however, the limiting frequency and associated coherence drop are robust against count rate and other factors. This argues in favour of high energy emission of a more stable special frequency. Given that in the disc, frequencies are strongly linked to radii, we must therefore look for special radii in the system at which abrupt changes are plausible.

There are three candidates for such a radius: the radius of the magnetosphere, the radius of the star, and the radius of the ISCO. In modern equations of state for dense matter (e.g. Akmal et al. 1998), the star is contained well inside the ISCO, especially for stars rotating at rates similar to 4U 1636−536. This argues against the stellar surface as a candidate for sharp frequency changes, simply because crossing the ISCO will surely produce dramatic effects (indeed, highly coherent oscillations should be impossible inside the ISCO), and this crossing would occur at a lower frequency than that of an orbit at the stellar surface. The options are therefore the magnetosphere and the ISCO. It is difficult to rule out a magnetospheric explanation, because very close to the star the magnetic field could have a complicated geometry with effects that are difficult to anticipate. We do note that the coherence drop is extremely abrupt (a factor of 10 in quality factor over a 8 per cent change in frequency), which might not be expected from a magnetosphere unless the magnetic field is extremely stiff. None the less, this is a possibility.

The remaining possibility is that the ISCO drives the sudden drop in coherence. The sudden drop in coherence at a reproducible limiting frequency is one of the signatures expected for the ISCO (see, e.g. Kluźniak & Wagoner 1985; Miller et al. 1998). The frequency at which this occurs is also reasonable. The behaviour we see is therefore qualitatively and quantitatively consistent with expected effects of the ISCO. However, the complexity of the source behaviour and the lack of evidence for abrupt changes in the upper QPO as well as the lower QPO mean that it is difficult to draw definite conclusions as to the origin of the drop in quality factor. With those caveats, we now discuss the implication for the neutron star mass, if the observed drop is related to the ISCO.

Within the ISCO interpretation, but independent of any detailed models, we can estimate the mass of the star. Our observations suggest that the frequency of the lower QPO is bounded at ∼900 Hz, possibly implying that the frequency of the upper QPO is also limited to 900 Hz + $\nu_{\rm spin}/2$, or ∼ 1200 Hz (the highest upper QPO frequency observed is ∼1150 Hz). For a rapidly rotating star such as 4U 1636−536, which is likely to have a dimensionless angular momentum of $j \equiv cJ/GM^2 \approx 0.1$–0.2, the mass implied by an ISCO frequency of 1200 Hz is ≈1.9–2.1 $M_\odot$ (see Miller et al. 1998, for the applicable formulae). Such a mass, although high compared to most estimated neutron star masses, is consistent with the most current nucleonic equations of state with plausible three-body repulsion (see Akmal et al. 1998), and could have resulted from Eddington-level accretion for a few tens of millions of years on to a neutron star with initial mass of 1.4 $M_\odot$.

4 CONCLUSIONS

By analysing in a homogeneous way all the available archival observations, we have followed the quality factor and rms amplitude of the two kHz QPOs detected in 4U 1636−536. One striking feature of our findings is that, towards the highest frequency, we observe a behaviour which may be consistent with a signal originating close to the ISCO: a reproducible and abrupt drop in the coherence of the lower kHz QPO. This result was obtained because we were able, for the first time, to analyse a very large data set homogeneously with no a priori data selection. The potential importance of these results demands more accumulation of evidence, but if similar patterns are seen in other systems then the rapid timing capabilities of *RXTE* may indeed have allowed the discovery of a long-anticipated effect of strong gravity.

ACKNOWLEDGMENTS

We are very grateful to Gerry Skinner, Jean-Pierre Lasota and Wlodek Kluźniak for very helpful and stimulating discussions, during the preparation of this paper. We are thankful to Mariano Méndez for his very valuable comments on the results presented, and for sharing his expertise on QPO studies with us. We thank an anonymous referee for suggestions which helped to strengthen the results presented in this paper. MCM was supported in part by NSF grant AST 0098436 at Maryland. MCM also thanks the Theoretical Institute for Advanced Research in Astrophysics (Hsinchu, Taiwan) for hospitality during part of this work. This research has made use of data obtained from the High Energy Astrophysics Science Archive Research Center (HEASARC), provided by NASA's Goddard Space Flight Center.

REFERENCES

Akmal A., Pandharipande V. R., Ravenhall D. G., 1998, Phys. Rev. C, 58, 1804
Bardeen J. M., Press W. H., Teukolsky S. A., 1972, ApJ, 178, 347
Barret D., Olive J. F., Boirin L., Done C., Skinner G. K., Grindlay J. E., 2000, ApJ, 533, 329
Barret D., Kluźniak W., Olive J. F., Paltani S., Skinner G. K., 2005, MNRAS, 357, 1288
Berger M. et al., 1996, ApJ, 469, L13
Bloser P. F., Grindlay J. E., Kaaret P., Zhang W., Smale A. P., Barret D., 2000, ApJ, 542, 1000
Boirin L., Barret D., Olive J. F., Bloser P. F., Grindlay J. E., 2000, A&A, 361, 121
Di Salvo T., Méndez M., van der Klis M., 2003, A&A, 406, 177
Jonker P. G., Méndez M., van der Klis M., 2000, ApJ, 540, L29

Jonker P. G., Méndez M., van der Klis M., 2002, MNRAS, 336, L1
Kaaret P., Piraino S., Bloser P. F., Ford E. C., Grindlay J. E., Santangelo A., Smale A. P., Zhang W., 1999, ApJ, 520, L37
Kluźniak W., Wagoner R. V., 1985, ApJ, 297, 548
Kluźniak W., Michelson P., Wagoner R. V., 1990, ApJ, 358, 538
Méndez M., 2002, in Vahe G., Gurzadyan R. T., Jantzen R. R., eds, Proc. MGIXMM Meeting, The Ninth Marcel Grossmann Meeting. World Scientific Publishing, Singapore, p. 2319
Méndez M. et al., 1998a, ApJ, 494, L65
Méndez M., van der Klis M., van Paradijs J., 1998b, ApJ, 506, L117
Méndez M., van der Klis M., Ford E. C., Wijnands R., van Paradijs J., 1999, ApJ, 511, L49
Méndez M., van der Klis M., Ford E. C., 2001, ApJ, 561, 1016
Miller M. C., Lamb F. K., Psaltis D., 1998, ApJ, 508, 791
Misra R., Shanthi K., 2004, MNRAS, 354, 945
Olive J., Barret D., Gierliński M., 2003, ApJ, 583, 416
Smale A. P., Zhang W., White N. E., 1997, ApJ, 483, L119
Strohmayer T. E., Markwardt C. B., 2002, ApJ, 577, 337
van der Klis M., 2001, ApJ, 561, 943
van der Klis M., 2005, in Lewin W. & van der Klis M., eds, Compact Stellar X-ray Sources. Cambridge Univ. Press, in press
van Straaten S., van der Klis M., Méndez M., 2003, ApJ, 596, 1155–1176
Wijnands R. A. D., van der Klis M., van Paradijs J., Lewin W. H. G., Lamb F. K., Vaughan B., Kuulkers E., 1997, ApJ, 479, L141
Wijnands R. A. D., van der Klis M., Homan J., Chakrabarty D., Markwardt C. B., Morgan E. H., 2003, Nat, 424, 44
Zhang W., Lapidus I., White N. E., Titarchuk L., 1996a, ApJ, 469, L17
Zhang W., Lapidus I., White N. E., Titarchuk L., 1996b, ApJ, 473, L135
Zhang W., Smale A. P., Strohmayer T. E., Swank J. H., 1998, ApJ, 500, L171

This paper has been typeset from a TEX/LATEX file prepared by the author.